

# Production Rate Measurements of $^{70}\text{As}$ , $^{61}\text{Cu}$ and $^{43}\text{Sc}$ from Heavy Ion Reactions

Anthony M Miller, Gunnar M Brown, Jerome Gan, Graham F. Peaslee; University of Notre Dame

## Introduction

Most positron-emitting isotope production has been performed using light ions such as protons, deuterons, and in fewer cases alphas. High cross sections and low particle evaporation numbers typically contribute to high yields from MBq to GBq  $\mu\text{A}^{-1}$  within a half-life of bombardment. In some cases, convenient target material exists; 17.9 MeV protons on a liquid natural zinc target produce roughly 83 MBq  $\mu\text{A}^{-1}$  of  $^{61}\text{Cu}$  at saturation with no inseparable contaminants of concern<sup>[1]</sup>. In contrast, consider the production of  $^{70,71}\text{As}$ . Possible targets for light ion reactions are gallium, germanium, selenium, bromine, and krypton. None of which are monoisotopic or physically convenient. Additionally, the existence of  $^{73}\text{As}$  with a half-life of 80.30 days poses concern as a chemically inseparable contaminant. With heavier ions such as  $^6\text{Li}$ ,  $^{10,11}\text{B}$ ,  $^{12}\text{C}$ ,  $^{14}\text{N}$ ,  $^{16}\text{O}$ ,  $^{19}\text{F}$ ,  $^{28}\text{Si}$ ,  $^{32}\text{S}$ ,  $^{35,37}\text{Cl}$ , the selection of target materials widens and compound nuclei are proton rich, potentially bypassing undesirably long-lived isotopes near the valley of stability. Several heavy ion reactions are examined in this work for their application in producing medically useful  $^{43}\text{Sc}$  (3.891 h),  $^{70}\text{As}$  (52.6 m), and  $^{61}\text{Cu}$  (3.339 h).

## Methodology

Natural aluminum, cobalt, and titanium targets were used with thicknesses of 0.25, 0.10, and 0.50 mm, respectively. A Multi-Cathode Source of Negative Ions by Cesium Sputtering (MC-SNICS) was used to generate  $^{16}\text{O}$  and  $^{19}\text{F}$  beams which were accelerated by a 10 MV FN Tandem accelerator. A 90-degree analyzing magnet was used to select the 6+ charge state for both beams. On target currents ranged from 50 to 200 pA.



Figure 1-3: Cathode wheel for MC-SNICS (left). End cap with aluminum target (center). Beam spot on quartz scintillator (right – the outer ring is an optical artifact from the edge of the quartz target).

An electrically isolated and suppressed end station allowed for charge collection and integration (Figure 4). Current readings from suppressed faraday cup three feet before the target was used for comparison. Additionally, an iridium-coated scintillator facilitated beam tuning.

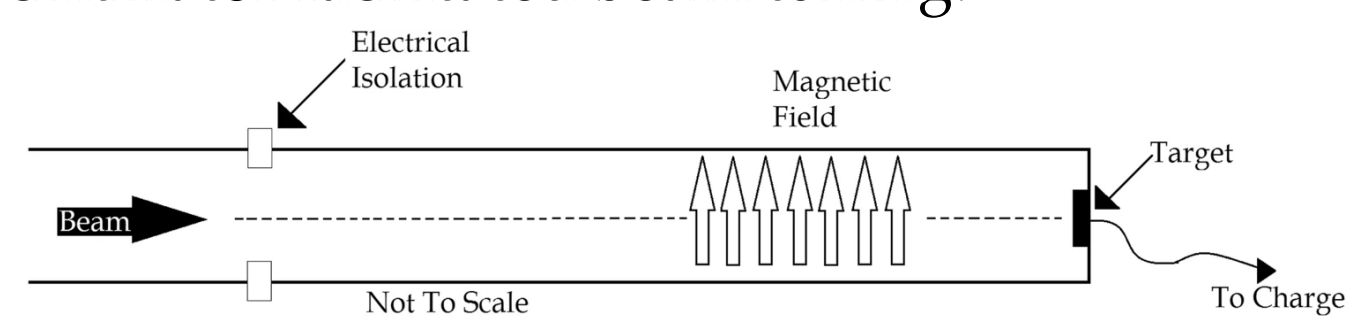


Figure 4: Electrically isolated end station with perpendicular magnetic field from permanent magnet. Figure from [2].

Offline gamma spectroscopy was performed with a fully shielded Canberra GC3518 and a partially shielded Canberra GC13023. A  $^{152}\text{Eu}$  source was used for energy calibrations while  $^{137}\text{Cs}$ ,  $^{133}\text{Ba}$ , and  $^{60}\text{Co}$  sources were used for detector efficiency estimations. Calibrations, peak fittings, and activity calculations were performed using the Fitzpeaks Gamma Analysis and Calibration Software—created by Jim Fitzgerald. LISE++ Utility: PACE4 and SRIM were used for cross section and stopping power estimations, respectively.

## Results and Conclusions

Table 1 summarizes the reactions tested. Irradiation time varied from fifteen to forty minutes—based on predicted production rates. After irradiation, the targets were allowed to cool for 30-min to an hour for safer handling and dead times below 10%. Data acquisition was based on ten-minute increments over several hours.



Figure 5: Partially shielded detector (left). Fully shielded detector in background (right).

For each spectrum obtained, a list of expected products from each reaction was generated based on the compound nucleus model, and PACE4 calculations. After considering half-life, a list of isotopes with their corresponding gamma emissions was used as fitting parameters in Fitzpeaks. A multi-day background spectrum allowed for the elimination of most unidentified peaks not accounted by the predicted nuclear reactions.

The identities of each of the isotopes were confirmed based on gamma energies, branching ratios, and half-life. End of bombardment activities were computed and used for production rate determination (Figures 6-8). Traces above and below the PACE4 prediction correspond to a 20% error in stopping power.

These production rates translate into saturation activities in Table 1. Note that average whole-body  $^{18}\text{F}$ -FDG PET scan requires 300-500 MBq of administrated activity<sup>[3]</sup>. Table 2 contains TENDL-based saturation activities of various light ion production methods for the isotopes of interest.

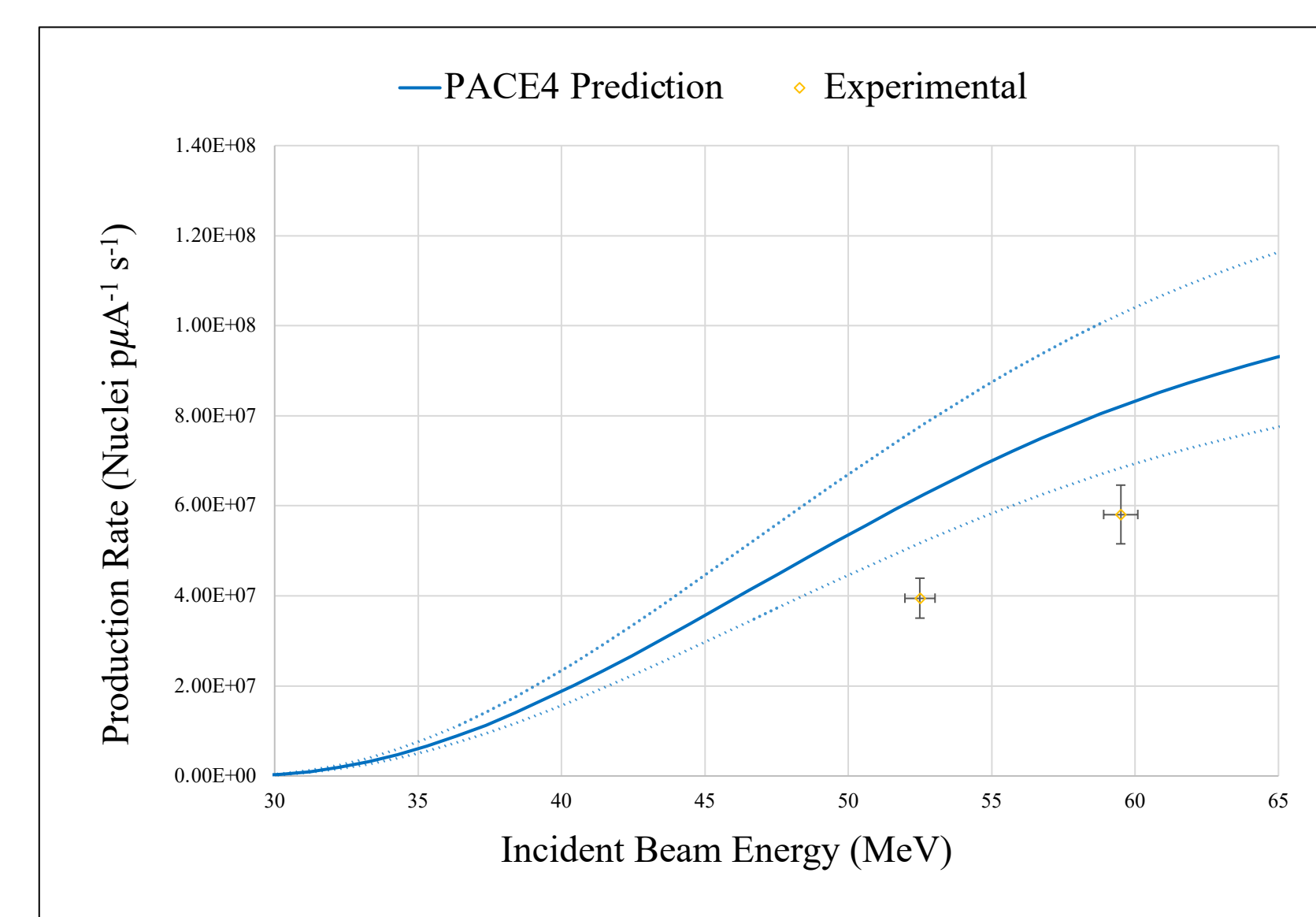


Figure 8:  $^{19}\text{F} + ^{27}\text{Al}$  Thick Target Production Rates of  $^{43}\text{Sc}$ . Detected by-products include:  $^{44,44m}\text{Sc}$ ,  $^{43}\text{K}$  (not shown).

Table 1: Saturation activities based on production rate measurements are provided for each nuclear reaction of interest along side the incident energies tested.

Nuclear Reaction	C.N.	Incident Energy (MeV)	Saturation Activity (MBq $\mu\text{A}^{-1}$ )
$^{59}\text{Co}(^{16}\text{O},\alpha\text{n})^{70}\text{As}$	$^{75}\text{Br}$	56.0	$14 \pm 1$
		50.4	$7.4 \pm 0.6$
		45.0	$3.8 \pm 0.3$
$^{\text{nat}}\text{Ti}(^{16}\text{O},\text{pxn})^{61}\text{Cu}$	$^{62-66}\text{Zn}$	56.0	$54 \pm 6$
		50.4	$35 \pm 4$
$^{27}\text{Al}(^{19}\text{F},\text{p2n})^{43}\text{Sc}$	$^{46}\text{Ti}$	59.5	$58 \pm 6$
		52.5	$40 \pm 4$

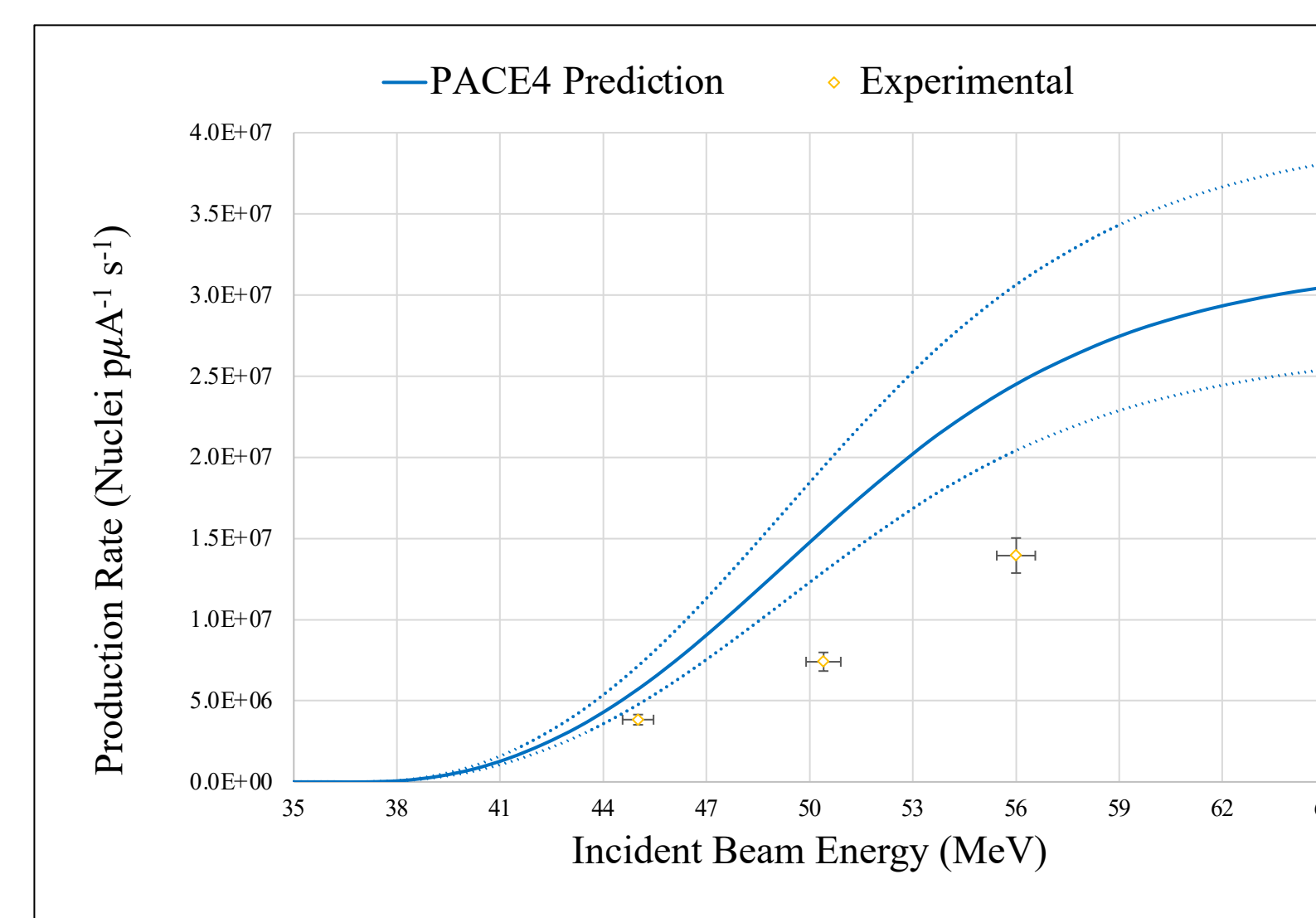


Figure 7:  $^{16}\text{O} + ^{59}\text{Co}$  Thick Target Production Rates of  $^{70}\text{As}$ . Detected by-products include:  $^{71}\text{As}$ ,  $^{75}\text{Se}$ ,  $^{69}\text{Ge}$  (not shown).

Table 2: Several light ion reactions on infinitely thick targets that are potentially viable for producing isotopes of interest. Incident energy was selected either by avoiding contaminant of concern ( $^{73}\text{As}$  and  $^{46}\text{Sc}$ )† or surpassing cross section maximum\*.

Isotope	Incident Energy (MeV)	Reaction	TENDL (MBq $\mu\text{A}^{-1}$ )
$^{70}\text{As}$	20	$^{70}\text{Ge}(p,n)$	7600
	25	$^{70}\text{Ge}(d,2n)$	4600
$^{43}\text{Sc}$	$^{16}\text{T}$	$^{\text{nat}}\text{Ca}(d,\text{xn})$	18.4
	16	$^{42}\text{Ca}(d,n)$	1800
	$^{20}\text{T}$	$^{\text{nat}}\text{Ca}(p,\text{xn})$	86
	20	$^{44}\text{Ca}(p,2n)$	3800
	$^{22}\text{T}$	$^{\text{nat}}\text{Ti}(p,2\text{pxn})$	102
	22	$^{46}\text{Ti}(p,\alpha)$	920
$^{61}\text{Cu}$	30*	$^{\text{nat}}\text{Zn}(p,2\text{pxn})$	1020

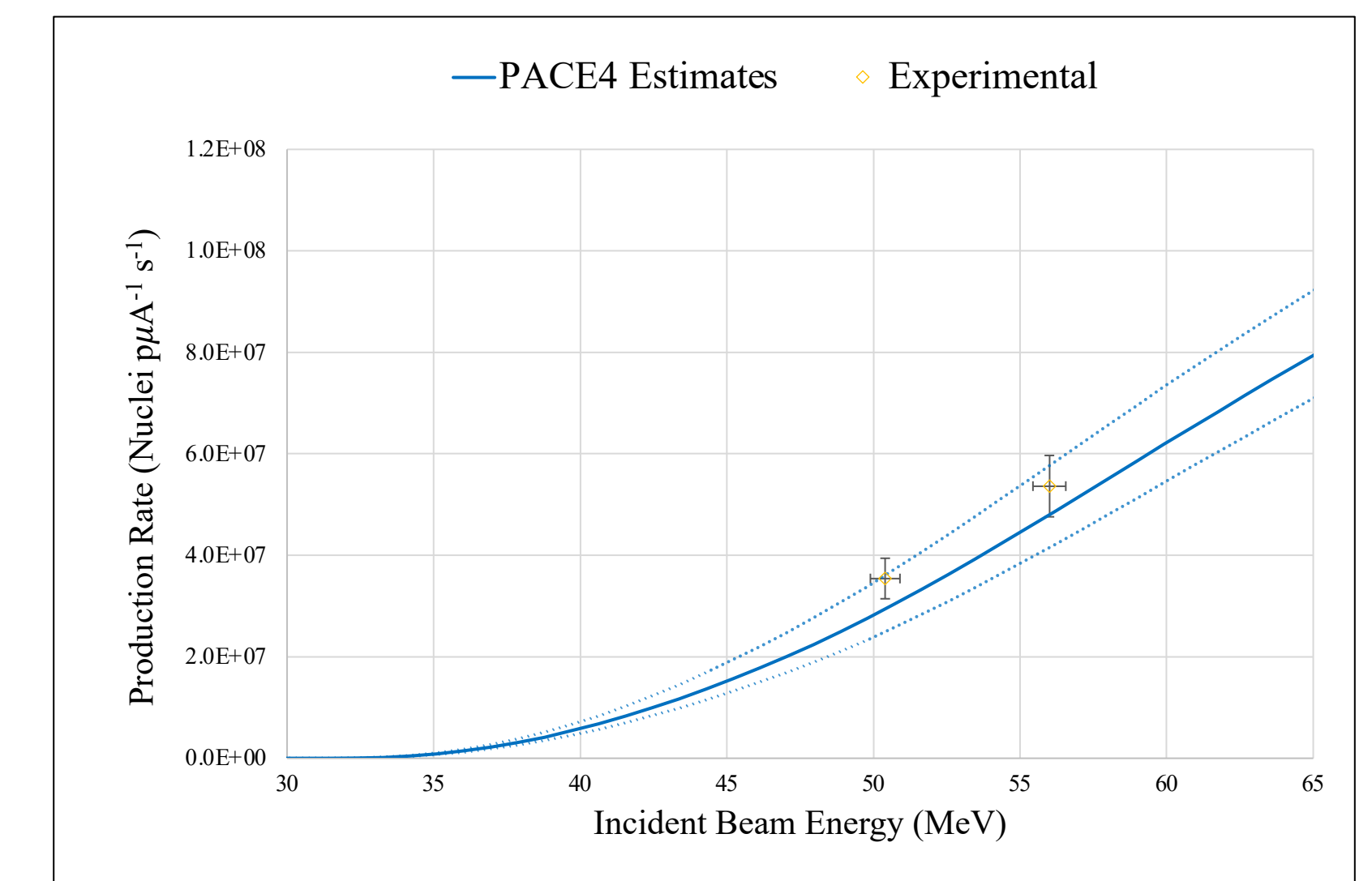


Figure 6:  $^{16}\text{O} + ^{\text{nat}}\text{Ti}$  Thick Target Production Rates of  $^{61}\text{Cu}$ . Detected by-products include:  $^{62}\text{Zn}$  (not shown).

A review of Tables 1 and 2 demonstrates the large difference in yield between light ions and heavy ion reactions. In some cases, such as  $^{61}\text{Cu}$ , inseparable long lived contaminants don't exist. Thus, the selection of energy hinges on cross section maxima and instrumentation. For  $^{43}\text{Sc}$  production with protons and deuterons on natural calcium, the avoidance of long-lived isotopes forces lower beam energies, cutting down yield. Alternatively, when enriched material may be used—the estimated yield increases significantly and allows for wider energy ranges to be used. However, enriched materials are costly and thus demand recycling.

Concerning  $^{59}\text{Co}(^{16}\text{O},\alpha\text{n})^{70}\text{As}$  and  $^{27}\text{Al}(^{19}\text{F},\text{p2n})^{43}\text{Sc}$ , useful activities may be generated provided sufficient current. Aluminum and cobalt are common metals and inexpensive. Both are naturally monoisotopic which reduces the production of undesired radioisotopes. Future work involves measuring production rates at higher beam energies, closely examining contaminants produced, and testing separation methods.

Data from  $^{59}\text{Co}(^{16}\text{O},\alpha\text{n})^{70}\text{As}$  measurements may be paired with data from a recent publication on producing  $^{76,77}\text{Br}$  using  $^{16}\text{O} + ^{\text{nat}}\text{Cu}$  [2]. With further investigation on the applicability of  $^{16}\text{O}$  beams, an argument for developing commercial cyclotrons capable of delivering several hundred  $\mu\text{A}$  of  $\sim 60$  MeV  $^{16}\text{O}$  beam may be formed.

For all heavy ion reactions, the reliability of Fusion-Evaporation codes such as PACE4 for heavy ions reactions remains uncertain<sup>[4]</sup>. The  $^{\text{nat}}\text{Ti}(^{16}\text{O},\text{pxn})^{61}\text{Cu}$  production rate measurement was the first in a series with increasing entrance channel mass and identical compound nuclei to explore mass asymmetry.

## Acknowledgments

John T. Wilkinson (LLNL), Jon Engle (UWM), Kaelyn Becker (UWM), Alyssa Wicks (ND), Robert Bartsch (ND).

Technical staff of the NSL, in particular Ed Stech.

ISNAP NSL, DOE funded HIPPO Program

## Literature cited

- S.J.C. do Carmo, et al. *Dalton Trans.* **46**, 14556 (2017)
- Sean R. McGuinness, et al. *Sci Rep* **11**, 15749 (2021)
- Adam L. Kesner, et al. *J. Am. Col. Radiology* **11**, 9, 920 (2014)
- Sean R. McGuinness, et al. *Nuc. Inst. Meth. Phys. Sec. B* **493**, 15 (2021)